

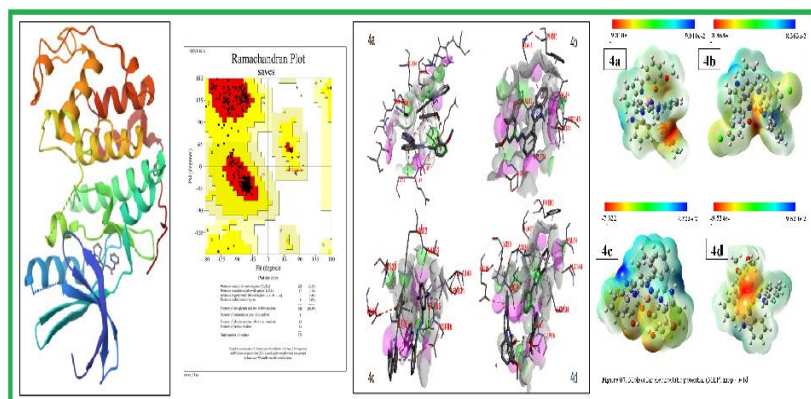
Full Paper | <http://dx.doi.org/10.17807/orbital.v17i1.22206>

Study of Copper Metallodrugs as Potential Inhibitor of Cancer via Molecular Docking and DFT

Gopal Krishna Murthy HR^a , Revanasidappa HD^a , Prema M^a , Mahendra Madegowda^b , Keshav Kumar Harish^b , Vasanth Kumar BC^c , and Sanjeevrayappa C^d 

Cancer remains a leading cause of mortality worldwide, demanding the development of novel therapeutic strategies. Recent advances in molecular biology and pharmacology have facilitated the discovery of new agents with potential anti-cancer activity. This study aims to elucidate the mechanisms underlying the anti-cancer effects of several newly identified compounds and assess their efficacy in preclinical models. As per literature, several compounds were screened for anti-cancer activity using a combination of *in-vitro* and *in-vivo* assays. In our research the *in-silico* analysis approach is used to explore the interactions between prepared compounds and Cyclin-Dependent Kinase 2 (CDK2), which is a crucial protein involved in cell cycle regulation and apoptosis. Immunohistochemistry will identify pathways involved in the compounds' anti-cancer effects. The study identified several compounds with a significant anti-cancer activity, demonstrating a dose-dependent inhibition of cancer cell proliferation and induction of apoptosis. Notably, our compounds exhibited the highest potency, leading to a substantial reduction in tumour growth in xenograft models.

Graphical abstract



Keywords

Cancer therapy
Novel compounds
Targeted therapy
Drug resistance
Anti-cancer agents

Article history

Received 06 Nov 2024
Revised 16 Apr 2025
Accepted 17 Apr 2025
Available online 03 May 2025

Handling Editor: Marcos S. Amaral

1. Introduction

Cancer continues to be one of the leading causes of death globally, with an estimated 10 million cancer-related deaths in 2020 alone [1]. The complexity of cancer biology, characterized by genetic mutations, epigenetic alterations and tumour microenvironment interactions, contributes to its persistence and resistance to conventional therapies [2].

Traditional treatments, including surgery, chemotherapy and radiation have significantly improved survival rates for many patients, but their effectiveness is often limited by side effects and the development of drug resistance [3].

^a Department of Chemistry, University of Mysore, Manasagangothri, Mysuru, Karnataka. ^b Department of Physics, University of Mysore, Manasagangothri, Mysuru, Karnataka. ^c Department of Chemistry, DRM College, Davanagere, Karnataka, India. ^d Department of Chemistry, GFGC, Yelahanka, Bangalore, Karnataka, India. *Corresponding author: gkmurthy123@gmail.com

In recent years, targeted therapies and immune-therapies have emerged as promising alternatives, offering more specific mechanisms of action against cancer cells while sparing normal tissues. Targeted therapies, such as tyrosine kinase inhibitors and monoclonal antibodies have shown significant success in treating cancers with specific genetic mutations or over expressed proteins [4]. Similarly, immune-therapies, including immune checkpoint inhibitors and CAR-T cell therapies have revolutionized the treatment of certain cancers by harnessing the body's immune system to target and destroy cancer cells [5]. Despite these advancements, challenges remain, including the development of resistance to targeted therapies and immunotherapy as well as the need for effective treatments for cancers with limited therapeutic options [6]. This highlights the importance of continued research into novel anti-cancer agents and therapeutic strategies. Natural products and synthetic compounds are being explored for their potential to offer new mechanisms of action and enhance the effectiveness of existing therapies [7]. Our study focuses on evaluating the anti-cancer activity of novel compounds, aiming to identify new agents with the potential to improve treatment outcomes. By investigating their mechanisms of action and efficacy in preclinical models, we seek to contribute to the development of more effective and less toxic cancer therapies.

Protein kinases classified as cyclin-dependent kinases (CDKs) are distinguished by their dependence on cyclin, a distinct component that supplies vital regions for their catalytic activity [8, 9]. These kinases are essential for controlling transcription and cell division in response to a variety of internal and external signals [10]. About thirty proteins with molecular weights ranging from 35 to 90 kDa make up the different family known as cyclins. The importance of the CDK family is highlighted by its participation in multiple signalling pathways that regulate transcriptional activities and the advancement of the cell cycle [11].

Most people believe that CDKs developed as a way to control the activity that promotes cell cycles in response to various stimuli and cellular circumstances. Due to their essential role in controlling the progression of the cell cycle and transcription inside cells, as well as their participation in apoptotic pathways, CDKs offer an attractive variety of targets for the development of innovative anticancer medications [11, 12]. Recently, there has been an increase in interest in copper complexes containing mixed ligands, including 1,10-phenanthroline, because of their strong DNA binding and cleaving activities, which show promise as anticancer agents via inducing apoptosis [12]. Based on this understanding, we have created copper compounds in the hopes of noticing strong anticancer effects. With a primary focus on CDK2 and four other synthetic complexes containing copper, this study attempts to evaluate the anticancer potential of these synthesized copper complexes.

2. Results and Discussion

2.1 Reference Target protein: Human Protein Kinase (PDB ID: 1gll). Ligand: Standard Drug - Ebvaciclib (CID: 134247638).

2.1.1 Docking Parameters (AutoDock Vina)

- Grid Box Center: x = 6.512, y = 15.587, z = 24.807
- Grid Box Size: 40 × 40 × 40 Å
- Exhaustiveness: 8
- Energy Range: 4 kcal/mol

2.1.2 Visualization

The docking output (.pdbqt) was visualized using PyMOL. The best docking pose was saved in .pdb format and further analyzed for interactions using BIOVIA Discovery Studio. The Figure 1 shows 3D representation of the molecular docking interaction between PDB ID: 1Gll (CDK4 mimic CDK2) and the standard anticancer drug Ebvaciclib. The ligand has shown bound within the ATP-binding pocket of the protein. Key hydrogen bond interactions are highlighted.

Optimal Pose: Binding Affinity: -8.1 kcal/mol, indicating a strong binding potential between Ebvaciclib and the 1gll protein target. Interaction Analysis (via BIOVIA Discovery Studio): In the best pose, the ligand formed key hydrogen bonds with the active site residues: Lysine 33 (LYS33) – H-bond donor to nitrogen in the ligand and Aspartate 145 (ASP145) – H-bond acceptor to hydroxyl group of the ligand. Additional hydrophobic interactions with residues such as Valine 64 (VAL64) and Leucine 83 (LEU83) further stabilized the ligand within the binding pocket.

The docking visualization shown in **Figure 1**, the Ebvaciclib snugly positioned in the active pocket of the 1gll protein, forming stabilizing hydrogen bonds with LYS33 and ASP145, key residues for kinase activity inhibition.[13]

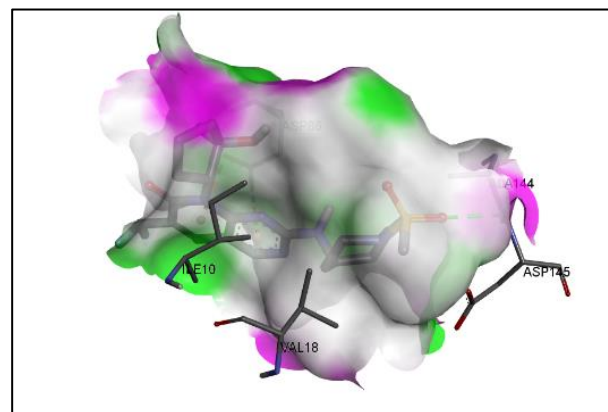


Fig. 1. 3D representation of the molecular docking.

The Table 1 shows, the most favourable binding pose with an affinity of **-8.1 kcal/mol**, suggesting that Ebvaciclib has better potential as an inhibitor of the 1gll protein, consistent with its known anticancer properties targeting CDK kinases.

Table 1. Binding affinity with Known anticancer target CDK kinase.

Mode	Binding Affinity (kcal/mol)	RMSD l.b.	RMSD u.b.
1	-8.2	0.000	0.000
2	-8.1	2.134	4.055
3	-7.9	2.549	3.021
4	-7.8	3.612	4.976
5	-7.8	4.841	8.810
6	-7.8	4.984	7.820
7	-7.7	3.974	6.169
8	-7.4	4.847	8.989
9	-7.3	3.027	4.201

2.2 Experimental Protein Structure Validation

The Protein cyclin dependent kinase features are as in the **Table 2**. The Ramachandran plot produced by PROCHECK RAMPAGE was used to validate the protein structures shown in **Figure 2**. The findings demonstrated that the residues were

found in the favourable and permitted regions, suggesting that the structure was appropriate for further molecular docking research. In this specific protein structure, the Ramachandran plot illustrates the energetically permissible regions for the backbone dihedral angles ψ vs. ϕ amino acid residues.

Table 2. Protein Features.

SI No	Protein Structure	Number of Residues in Favored Regions (%)	Number of Residues in Allowed Regions (%)	Number of Residues in Disallowed Regions (%)
1	Cyclin dependent kinase 2 (1GII)	92.5	7.1	0.0

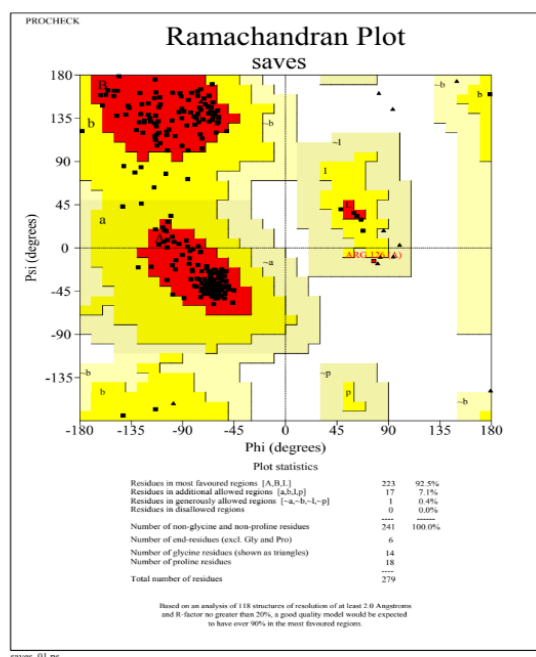


Fig. 2. The Ramachandran plot generated from RAMPAGE.

2.2.1 Protein-Ligand Interaction

The summary of the results obtained from the molecular docking studies conducted between the selected protein and the synthetic compounds are shown in **Table 3**. Based on the lowest binding affinity values [Kcal/mol], the ideal docking pose for each compound was identified. We used BIOVIA Discovery Studio Visualizer software to clarify the interactions between the chosen ligands and the protein.

Table 3. Molecular Docking results (Binding energy value δG is shown in minus kcal/mol).

Protein Name	Compounds Name	Binding Affinity (kcal/mol)
Cyclin-dependent kinase 2 (1GII)	4a	-11.00
	4b	-9.94
	4c	-10.64
	4d	-10.24

2.2.2 Analysis of Selected protein and synthetic compound Interactions

Molecular docking studies conducted between the selected protein and synthetic compounds interactions revealed the relationship between the ligands and the protein. The Compound 4a demonstrated the strongest binding affinity, as indicated by the highest binding score, as shown in **Table 4**. Following analysis with the BIOVIA Discovery software showed that in the Cyclin-dependent kinase 2 (1GII), both 4a and 4b formed three hydrogen bonds with important amino acid residues.

Table 4. No. of Hydrogen bonds between ligands and selected protein.

Protein Name	Compound Name	Number of Hydrogen bonds	Residue name
Cyclin-dependent kinase 2 (1GII)	4a	3	ILE10, GLU12, ASP86
	4b	3	VAL83, ASP86, ASP145
	4c	2	HIS82, VAL83
	4d	1	ASP86

The Molecular docking studies using Autodock Vina were able to visualize in three dimensions the binding interactions that occur between ligands and proteins. In particular, compounds 4a and 4b demonstrated encouraging interactions with the target protein, establishing hydrogen bonds with the previously mentioned active amino acid residues. The findings indicate that these compounds, a synthetic copper compound, may interact with Cyclin-Dependent Kinase 2 and could be affecting its activity.

The **Figure 3** shows the 3D-visualisation of Cyclin-dependent kinase 2 (1GII) protein docked with novel ligands 4a, 4b, 4c and 4d showing amino acid interactions.

2.3 Frontier molecular orbital and molecular electrostatic potential analysis

Combining molecular docking with DFT calculations can enhance the understanding of ligand-receptor interactions. After docking a ligand to a target protein, DFT can be used to refine the ligand's conformation and calculate the binding energy more accurately.

In **Figure 4**, the HOMO (Highest Occupied Molecular Orbital) energy is similar to the trend of ionization potential, while the LUMO (Lowest Unoccupied Molecular Orbital) energy indicates the electron affinity.[16]

The energy gap is crucial in determining the electronic properties such as chemical reactivity and kinetic stability (19,20). The total energies (E) for the alpha and beta spin states indicate the stability of the molecules (22). Among the four compounds, 4a shows the lowest total energy of 1.81 and 1.37eV suggesting it is the most stable among four, particularly for the alpha spin state. Accordingly compound 4d has the lowest HOMO energy (-5.78 eV for alpha spin), making it the hardest to ionize among the compounds. The LUMO energy is also lowest for 4d (-2.34 eV for alpha spin), indicating it has a stronger affinity for accepting electrons. Thereby 4d exhibiting the largest energy gap (3.44 eV for alpha spin), implying it is the most chemically stable and less reactive. On the contrary, 4a shows the smallest gap (1.81 eV for alpha spin), indicating higher chemical reactivity. The complete details of the other chemical descriptor parameters are shown in Table 5. The ionization potential follows the same trend as the HOMO energy. 4d has the highest ionization

potential (5.78 eV for alpha spin), making it the most resistant to ionization. Electron affinity trends similarly to LUMO energy, 4d has a higher electron affinity (2.34 eV for alpha spin), making it more likely to accept electrons. Further it is also observed that 4d is the hardest compound ($\eta = 1.72$ eV for alpha spin), meaning it is less reactive, while 4a is the softest ($\eta = 0.905$ eV for alpha spin), making it more reactive. The molecule 4a results with greater chemical potential for its alpha spin implying a greater tendency to accept electrons and also greater electrophilicity index to describe its

potentiality as a potent electrophile. The corresponding data has been shown in **Table 5**.

Among the four compounds, 4d stands out as the most stable due to its highest ionization potential, largest energy gap, and greatest global hardness. This makes 4d the least reactive and most chemically stable option. On the other hand, 4a is the most reactive, characterized by its smallest energy gap, highest chemical potential, and greatest electrophilicity, making it the best choice due to reactivity.

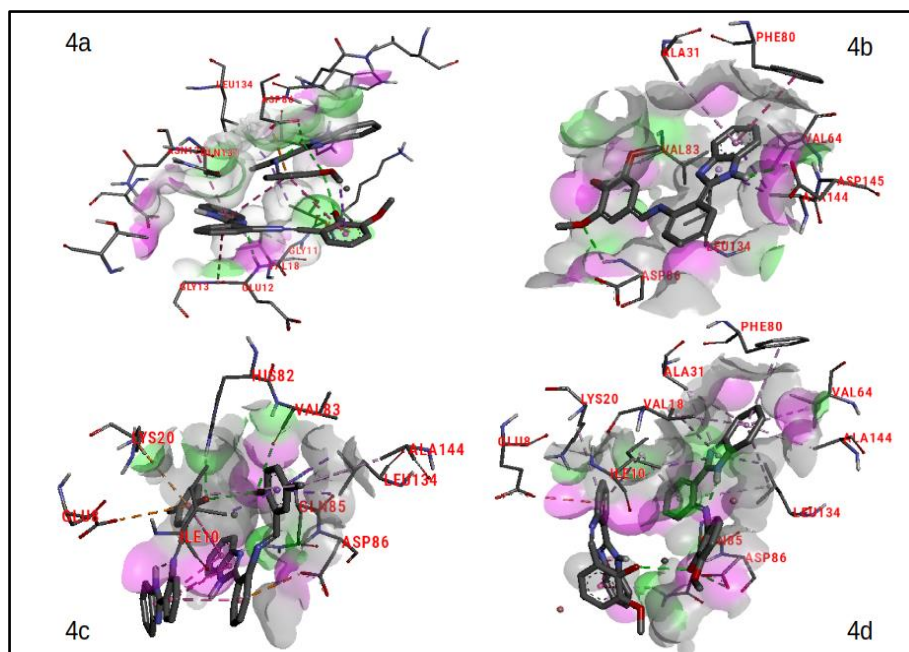


Fig. 3. 3D- visualisation of protein docked with novel ligands.

Table 5. GCRD properties of Effective 4a to 4d copper metal complexes.

GCRD Properties	Symbol / Formula	4a		4b		4c		4d	
		Alpha	Beta	Alpha	Beta	Alpha	Beta	Alpha	Beta
Energy	E (a. u.)	-3889.31		-2244.68		-2391.56		-2037.19	
E _{HOMO}	E _H (eV)	-4.02	-4.00	-5.22	-5.16	-5.26	-5.22	-5.78	-5.76
E _{LUMO}	E _L (eV)	-2.20	-2.62	-1.97	-2.25	-2.14	-2.58	-2.34	-2.74
ΔE _{LUMO-HOMO}	E _g =E _{L-H} (eV)	1.81	1.37	3.25	2.91	3.11	2.64	3.44	3.01
Ionization potential(I)	I = - E _H (eV)	4.02	4.00	5.22	5.16	5.26	5.22	5.78	5.76
Electron affinity (A)	A = - E _L (eV)	2.20	2.62	1.97	2.25	2.14	2.58	2.34	2.74
Global Hardness (η)	η= (E _{L-H})/2 (eV)	0.905	0.685	1.625	1.455	1.555	1.32	1.72	1.505
Softness (S)	S= 1/2η(eV ⁻¹)	0.552	0.729	0.307	0.343	0.321	0.378	0.290	0.332
Chemical potential(μ)	μ =(E _H +E _L)/2 (eV)	5.12	3.31	3.59	3.70	3.7	3.9	4.06	4.25
Electronegativity (χ)	χ = - μ (eV)	-5.12	-3.31	-3.59	-3.70	-3.7	-3.9	-4.06	-4.25
Electrophilicity (ψ)	ψ = μ ² /2 η (eV)	14.47	7.986	3.956	4.695	4.394	5.749	4.780	5.996

The molecular electrostatic potential (MEP) maps are useful for understanding the distribution of electrostatic potential across the surface of the molecules, which can indicate regions of electron density, potential sites for nucleophilic and electrophilic attacks, and help in predicting the reactivity and interaction of the molecules with other entities, like enzymes or receptors. Red regions on the map indicate areas of high electron density (negative electrostatic potential), usually associated with electronegative atoms (like oxygen or nitrogen). These areas are likely to attract positively

charged species (nucleophiles). Similarly blue regions indicate areas of low electron density (positive electrostatic potential), usually around electropositive atoms (like hydrogen). These areas are likely to attract negatively charged species (electrophiles). Green, yellow, and orange regions indicate intermediate levels of electrostatic potential.

The MEP maps of all the four complex compounds as shown in **Figure 4**. It is observed from the figure that molecule 4a resulted with highest potential in the range of $\pm 9.810 \times 10^{-2}$ when compared others. In all the complexes it is observed that

the red regions are indicated near oxygen atoms indicating negative electro potential probing to attacking nucleophiles. The combination of molecular docking and DFT calculations provides a powerful toolkit for exploring the interactions of chemical ligands with biological targets. This approach not

only aids in predicting binding affinities but also enhances the understanding of the electronic properties of ligands, ultimately contributing to the rational design of new therapeutic agents.

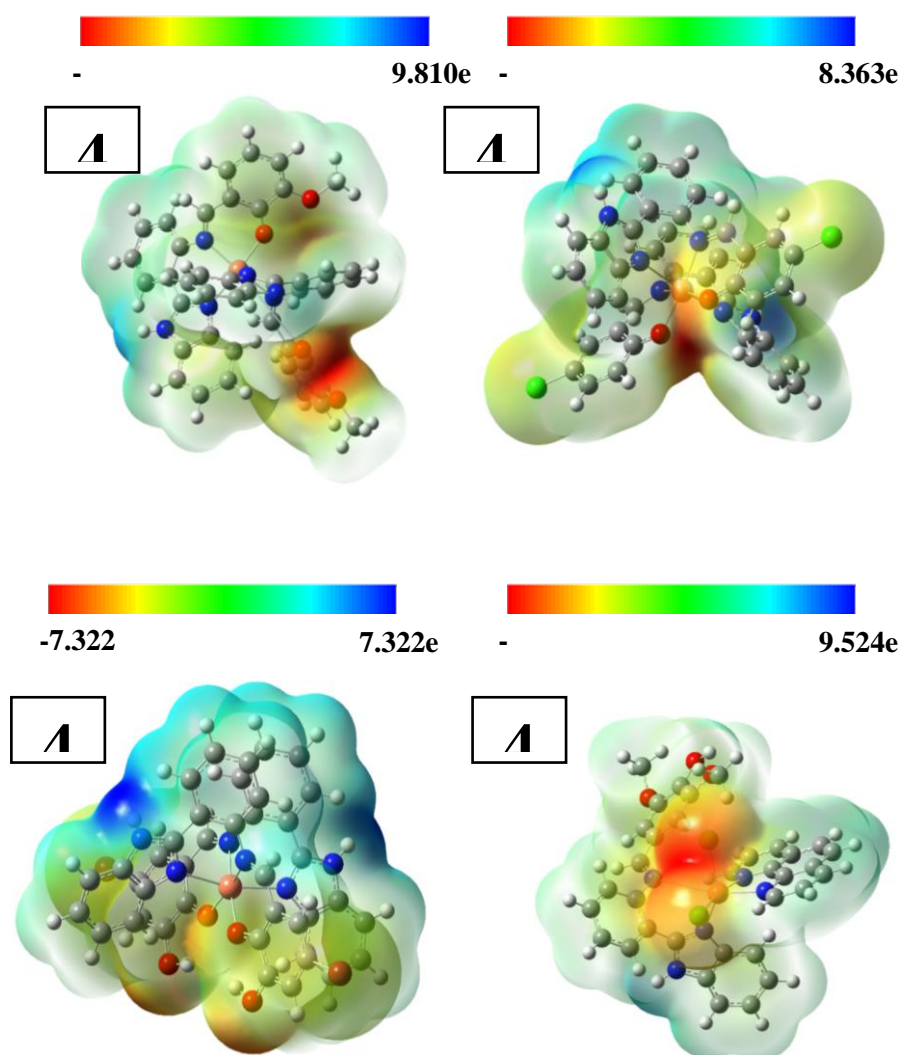


Fig. 4. Molecular electrostatic potential (MEP) map 4a to 4d.

2.4 Discussion

The objective of our study was to assess the anticancer potential of newly synthesized compounds and find their interaction with an anticancer protein target Cyclin-dependent kinase 2. As Cyclin-dependent kinase plays a crucial role in cancer biology. It primarily regulates cell cycle progression and influences various oncogenic signalling pathways. Cyclin-dependent kinase 2 [CDK2] functions as a serine/threonine kinase, that is activated through its interaction with cyclins [Cyclin A and Cyclin E]. Upon activation, CDK2 phosphorylates key substrates, like the transcription factors SMAD3, FOXM1, and MYC, which are integral to cell cycle progression and oncogenesis.

Elevated levels of CDK2 and its cyclin partners have been linked to various cancers like breast, ovary and prostate [18]. CDK2 has become a potential target for anticancer treatments due to its crucial involvement in cancer progression. Our study focuses on newly synthesized copper mixed synthetic compounds show optimal biological activity by employing

advanced bioinformatics tools and software, the study conducted a comprehensively *in-silico* evaluation of four synthesized compounds against Cyclin-dependent kinase 2.

The active site of CDK2 comprises specific amino acid residues, predominantly hydrophobic such as 31 Alanine, 144 Alanine, 132 Asparagine, 86 Aspartic acid, 145 Aspartic acid, 85 Glutamine, 131 Glutamine, 81 Glutamic acid, 84 Histidine, 10 Isoleucine, 134 Leucine, 33 Lysine, 80 Phenylalanine, 18 Valine, 64, 83 Valine play a crucial role in receptor-ligand interactions.

In a related study, the known CDK2 inhibitor Ebvaciclib considered as a positive control in the evaluation of the synthesized pteridin-7(8H)-one derivative. The study compares the potency and selectivity of the new compounds against CDK2 with that of Ebvaciclib, highlighting the potential of the newly developed inhibitors in relation to this established drug [19].

A series of novel pteridin-7(8H)-one derivative was synthesized and evaluated as potential CDK2 inhibitors, with

a particular emphasis on comparing these results with the well-characterized CDK2 protein structure of PDB ID 1GII. The 1GII structure, which depicts CDK2 in complex with a known inhibitor (Ebvaciclib), serves as a valuable reference for understanding how various inhibitors engage with the CDK2 active site.

Our analysis showed that the newly synthesized compounds, particularly 4a and 4c, exhibit selective and potent inhibition of CDK2 with binding affinity -11 and -10.64, paralleling the findings observed with compound KII-21. The binding interactions such as hydrogen bond and hydrophobic pockets are similar in these compounds with those seen in the 1GII structure, where critical interactions at the kinase's active site, particularly involving polar groups at the 6-position of the pteridine ring [a bicyclic heterocyclic system made up of a pyrimidine ring and a pyrazine ring], are vital for optimal binding affinity. This comparison highlights the importance of precise molecular interactions for achieving selective CDK2 inhibition.

Targeting CDK2 is significant due to its central role in cell cycle regulation, particularly during the transition from the G1 to S phase, which is essential for cell proliferation. By selectively inhibiting CDK2, from similar study KII-21, shown promise in disrupting cancer cell proliferation with minimized off-target effects, making them strong candidates for further drug development. The structural parallels and distinctions observed between our compounds and the CDK2 structure in 1GII provided valuable insights for ongoing optimization efforts aimed at developing more effective and selective CDK2 inhibitors. The current study suggests that the novel compounds may have potential anticancer activity. Future *in vitro* research should focus on clarifying their effects on various cancer-related targets.

3. Material and Methods

3.1 The Reference Protein Target

Human Protein Kinase (PDB ID: 1gII) and Standard Drug - Ebvaciclib (CID: 134247638)

3.1.1 Ligand Preparation

Ebvaciclib was downloaded in 3D SDF format from PubChem (CID: 134247638), then converted to .pdbqt format using AutoDock Tools after ensuring proper hydrogen addition and torsional flexibility.

3.1.2 Protein Preparation

The crystal structure of the protein (PDB ID: 1gII) was retrieved from the RCSB Protein Data Bank. Water molecules, native ligands, and non-essential chains were removed. The protein structure was cleaned and prepared for docking by adding polar hydrogens and assigning Gasteiger charges using AutoDock Tools and saved in .pdbqt format.

3.2. Synthesized Ligands and Protein

3.2.1 The synthesized ligands

The synthesized ligands from our laboratory were considered for the present studies. The canonical SMILES of the collected ligands (synthesized compounds) were entered into the Swiss Target Prediction database to obtain the corresponding target genes.

The Ligands used with copper metal are L1 and L2, L3 and L4 [L1 to L4] are shown in the Figure 5 and 6, respectively.

L1: 2 - (5,6-dihydro-benzo [4,5] imidazo [1,2-c]quinazolin-6-yl)6-methoxy phenol.

L2: 4 - (5,6-dihydro-benzo [4,5] imidazo [1,2-c]quinazolin-6-yl) 2,6-dimethoxy phenol.

L3: 4-chloro-2- (5,6-dihydro-benzo [4,5] imidazo [1,2-c]quinazolin-6-yl) phenol.

L4: 4 bromo-2- (5,6-dihydro-benzo [4,5] imidazo [1,2-c]quinazolin-6-yl) 6-methoxy phenol.

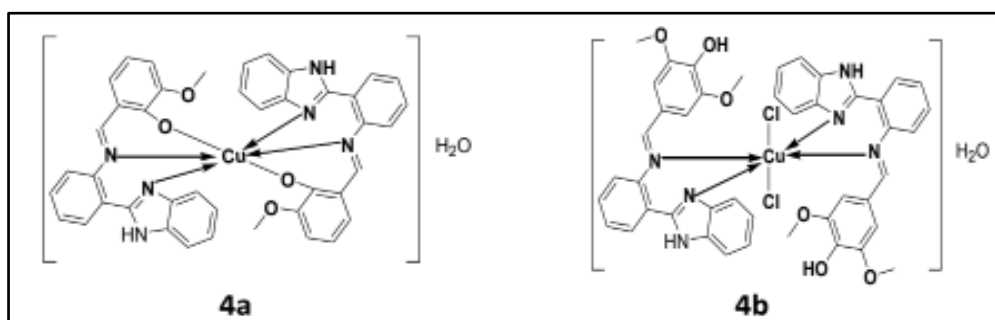


Fig. 5. Representation of synthesized 4a and 4b.

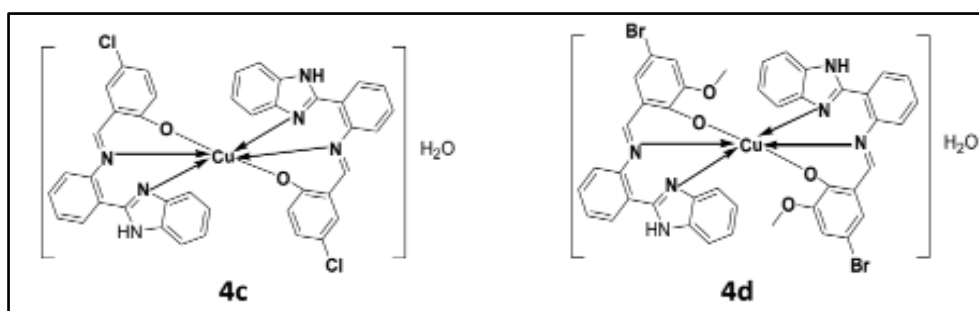


Fig. 6. Representation of synthesized 4c and 4d.

3.2.2 Selection of Protein

Based on the comprehensive literature review, we were able to identify a protein from the selectively-listed papers, from Protein Data Bank (PDB) with Id 1GII is chosen as the target cyclin-dependent kinase 2 in **Figure 7**. By the results of earlier investigations, this specific protein was selected because of its known anticancer properties.

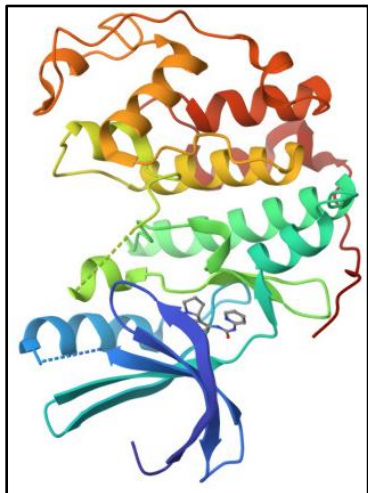


Fig. 7. 3D-Structure of Cyclin-dependent kinase 2 (1GII) from PDB.

3.2.3 Preparation of Ligand and Protein

Ebvaciclib was downloaded in 3D SDF format from PubChem (CID: 134247638), then converted to .pdbqt format using AutoDock Tools after ensuring proper hydrogen addition and torsional flexibility.

Cyclin-dependent kinase 2 of (PDB ID -1GII) three-dimensional structure was obtained from the Protein Data Bank (PDB) (46). PyMOL is a robust open-source software for molecular visualization, widely utilized in fields such as structural biology, and computational chemistry [14]. The crystal structure of the protein (PDB ID: 1gii) was retrieved from the RCSB Protein Data Bank. Water molecules, native ligands, and non-essential chains were removed. The protein structure was cleaned and prepared for docking by adding polar hydrogens and assigning Gasteiger charges using AutoDock Tools and saved in .pdbqt format.

3.2.4 Prediction of Binding Site

To study the revised structure for finding the possible binding sites on protein, the *in-silico* tool CASTp was utilized. The areas of the protein were found based on interaction of ligand with the protein, which demanded careful investigation [15].

3.2.5 Validation of Protein Structure

The Ramachandran plot generated by the PROCHECK RAMPAGE tool in UCLA-DOE LAB-SAVES v6.0 was used to validate the structure of cyclin-dependent kinase 2 (1GII). The findings validated the protein structure's validity and stability.

3.2.6 Molecular Docking Visualization

Molecular docking interactions between the ligands and proteins was studied using BIOVIA Discovery Studio Visualizer. This software is useful to create 3D visualizations

that highlighted important interactions like bond lengths, hydrophobic interactions, and hydrogen bonds.

3.2.7 Molecular Docking Visualization

With the use of BIOVIA Discovery Studio Visualizer, the docking interactions between the ligands and proteins are able to be visually presented. With the use of this software, it was possible to create 3D visualizations that highlighted important interactions such bond lengths, hydrophobic interactions, and hydrogen bonds.

3.2.8 Density Functional Theory

Gaussian09 was used to carry out DFT studies for the lead compounds 4a to 4d. The molecular structures of L1 to L4 were created and examined with Gauss View 5. The geometries were optimized at the B3LYP level with a lan12dz basis set [17].

4. Conclusions

In this work, synthetic compounds containing copper has revealed intriguing properties that may help to fight cancer. Compound 4a, 4b, 4c and 4d demonstrate significant interaction binding energy -11.00, -9.94, -10.64 and -10.24 (kcal/mol) respectively with the anticancer target protein CDK2 [Cyclin Dependent Kinase 2]. The compound 4a has shown the best binding energy value signifying the importance in cancer treatment like targeting cell cycle regulation and apoptosis. The ability of these compounds to form strong binding affinities with Cyclin Dependent Kinase 2 is attributed to their interaction with active site residues and nearby atoms. So, all the compounds 4a, 4b, 4c and 4d has shown better binding affinity values compared to the Reference protein–ligand binding affinity, which was shown -8.2. Although more research is necessary to confirm the effectiveness of these findings, they do mark a significant advancement in the development of a more effective anticancer activity. In future research, the Absorption, Distribution, Metabolism, Excretion/Toxicity [ADME/T] characteristics of these compounds could be evaluated through wet lab experiments.

Acknowledgments

The author GKM take this opportunity to thank to the Department of Collegiate Education and University of Mysore for the encouragement for Research. The author Keshav Kumar Harish would like to acknowledge DST-KSTePS, Government of Karnataka for providing fellowship.

Author Contributions

GKMHR -Literature survey, Data collection, Analysis, Molecular docking. RHD and PM - Paper correction as supervisor. MM and KH – Paper draft, DFT. VKBC - Synthesis of ligands and metal complexes. SC - Study of bio-activity.

References and Notes

- [1] Sung, H.; Ferlay, J.; Siegel, R. L.; Laversanne, M.; Soerjomataram, I.; Jemal, A. *CA Cancer J. Clin.* **2021**, *71*, 209. [\[Crossref\]](#)

- [2] Hanahan, D.; Weinberg, R. *Cell* **2022**, 185, 2656. [\[Crossref\]](#)
- [3] Dai, H.; Zhang, W.; Li, J.; *Cancer Letters* **2023**, 546, 215. [\[Crossref\]](#)
- [4] Rexer, B. N.; Arteaga, C. L. *Mol. Cancer Ther.* **2023**, 22, 1. [\[Crossref\]](#)
- [5] Lurain, K.; Ramaswami, R.; Ekwede, I.; Goyal, G.; Menon, M.; Odeny, T. A.; et al. *J. Clin. Oncol.* **2024**, 56, 2. [\[Crossref\]](#)
- [6] Joshi, V. B.; Spiess, P. E.; Necchi, A.; Pettaway, C. A.; Chahoud, J. *Nat. Rev. Urol.* **2022** 19, 457. [\[Crossref\]](#)
- [7] Newman, D. J.; Cragg, G. M.; *J. Nat. Prod.* **2023**, 86, 1. [\[Crossref\]](#)
- [8] Kciuk, M.; Gielecińska, A.; Mujwar, S.; Mojzych, M.; Kontek, R. *Biochim. Biophys. Acta BBA – Rev. Cancer* **2022**, 1877, 188716. [\[Crossref\]](#)
- [9] Ding, L.; Cao, J.; Lin, W.; Chen, H.; Xiong, X.; Ao, H. *Int. J. Mol. Sci.* **2020**, 13, 1960. [\[Crossref\]](#)
- [10] Łukasik, P.; Załuski, M.; Gutowska, I. *Int. J. Mol. Sci.* **2021**, 13, 2935. [\[Crossref\]](#)
- [11] Chou, J.; Quigley, D. A.; Robinson, T. M.; Feng, F. Y.; Ashworth, A. *Cancer Discov.* **2020**, 10, 351. [\[Link\]](#)
- [12] Kathiresan, S.; Muges, S.; Annaraj, J.; Murugan, M. *New J. Chem.* **2017**, 41, 1267. [\[Crossref\]](#)
- [13] Ikuta, M.; Kamata, K.; Fukasawa, K.; Honma, T.; Machida, T.; Hirai, H.; Suzuki-Takahashi, I.; Hayama, T.; Nishimura, S. *J. Biol. Chem.* **2001**, 276, 27548. [\[Crossref\]](#)
- [14] Mooers, B. H. M.; Brown, M. E. *Protein Sci.* **2021**, 30, 262. [\[Crossref\]](#)
- [15] Tian, W.; Chen, C.; Lei, X.; Zhao, J.; Liang, J. *Nucleic Acids Res.* **2018**, 2, W363. [\[Crossref\]](#)
- [16] Kumar, K. H.; Ananda, S.; Dukanya.; Keerthikumara, V.; Basappa; Mahendra, M. *IOP Conf. Ser.: Mater. Sci. Eng.* **2024**, 1300, 012007. [\[Link\]](#)
- [17] Bharathi, A. K.; Jeyaseelan, C. S.; Hussain, S.; Benial, A. M. F. *Spectrochim. Acta A Mol. Biomol. Spectrosc.* **2023**, 5, 123074. [\[Crossref\]](#)
- [18] Harish, K. K.; Nesaragi, A. R.; Kalagatur, N. K.; Naik, P.; Madegowda, M.; Pandith, A. *J. Photochem. Photobiol. Chem.* **2024**, 452, 15565. [\[Crossref\]](#)
- [19] Tadesse, S.; Caldon, E. C.; Tilley, W.; Wang, S. *J. Med. Chem.* **2019**, 62, 4233. [\[Crossref\]](#)

How to cite this article

Gopal, K. M. H. R.; Revanasidappa, H. D.; Prema, M.; Mahendra, M.; Keshav, K. H.; Vasanth, K. B. C.; Sanjeevrayappa, C. *Orbital: Electronic J. Chem.* **2025**, 17, 107. DOI: <http://dx.doi.org/10.17807/orbital.v17i1.22206>